Coastal Engineering 183 (2023) 104328

Contents lists available at ScienceDirect

Coastal Engineering

journal homepage: www.elsevier.com/locate/coastaleng

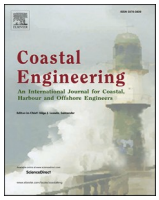

Reductions in water level over coastal wetlands during storm surges and tsunamis: An analytical result and a critical review of the literature

Alastair Grant [a,*], Mark J. Cooker [b]

[a] School of Environmental Sciences, University of East Anglia, Norwich, NR4 7TJ, UK
[b] School of Mathematics, University of East Anglia, Norwich, NR4 7TJ, UK

ARTICLE INFO

Keywords:
Coastal protection
Wetland
Saltmarsh
Mangrove
Storm surge
Tsunami

ABSTRACT

Understanding how saltmarshes and mangroves reduce movement inland of high water levels resulting from storm surges and tsunamis is vital for disaster planning and predicting impacts of sea level rise. This has been examined using both site-specific hydrodynamic models and field measurement, but an overarching theoretical framework is lacking. To address this, we provide a simple analytical solution for the propagation of a surge across a uniform wetland surface. The distance that flooding penetrates inland is reduced by the presence of vegetation and increases with both surge height and duration. After 4 h, 1 m and 5 m floods will travel 5.5 and 19.1 km inland over saltmarshes respectively. Penetration distances are approximately 2.5 times smaller for mangroves and are lower for short duration events, emphasising the effectiveness of mangroves in reducing impacts of tsunamis. The (absolute) reduction in water level per km depends strongly on surge duration and vegetation type, but only weakly on surge height. In a surge rising by 2m over 1 h, the reduction in water level over a saltmarsh can be as high as 45 cm/km, but reduces as surge duration increases or where the width of the low-lying land is small enough for the surge to fill "the bathtub". So water level reductions will be greatest during short duration events or when large widths of wetland are maintained. Several studies report much higher rates of attenuation, but these involve up to 50-fold extrapolation from measurements made over short distances or misinterpretations of primary sources. Once these are excluded, field data are consistent with our model results.

1. Introduction

Many coastal communities and economic assets are vulnerable to flooding. Flood risks are increasing as a result of sea level rise (c.f. Kirezci et al., 2020; Kulp and Strauss, 2019) and potential greater frequency of extreme storm events (Garner et al., 2017; Rahmstorf, 2017). A number of studies have argued that wetlands provide protection against coastal flooding, as a consequence of both wave energy dissipation (Figueroa-Alfaro et al., 2022; Maza et al., 2022; Pinsky et al., 2013; Zhang et al., 2022) and slowing of the rate that unusually high water levels are able to penetrate inland (Barbier et al., 2013; Kiesel et al., 2019, 2022; Leonardi et al., 2018; Paquier et al., 2017; Stark et al., 2015). These flood protection ecosystem services make a substantial contribution to estimates of the economic value of coastal wetlands (Barbier, 2007). There has been some argument about the true importance of these processes (Gedan et al., 2011), including discussion of the extent to which flood protection results from the presence of vegetation directly; or via an indirect mechanism, whereby vegetation stabilises sediment at a higher elevation than would occur without vegetation (Feagin, 2008). Elsewhere, we have argued that importance of wave attenuation by wetlands during storm surges has been overstated (Alotaibi and Grant, Submitted). Here we examine the extent to which wetlands lead to a reduction in water level as one moves inland during a storm surge. We do not consider wave attenuation here, although the theory does give some insights into the extent to which wetlands will protect against coastal flooding during a tsunami.

Empirical studies reviewed by Gedan et al. (2011) reported reductions in water depth varying between 4.4 cm/km and 16.6 cm per km (values given in text – their Figure 7a shows a larger range than this). Leonardi et al. (2018) give a range of 1.7–25 cm/km and Krauss et al. (2009) report one value of 18.9 cm/km with all others were between 4.2 and 9.4 cm/km. But more recent studies have reported reductions of water level as large as 100 cm/km (Kiesel et al., 2019) or even 270 cm/km (Paquier et al., 2017). A number of authors have used hydrodynamic modelling to make predictions of storm surge behaviour at particular locations (Hu et al., 2015; Resio and Westerink, 2008; Stark

* Corresponding author. School of Environmental Sciences, University of East Anglia, Norwich, NR4 7TJ, UK.
E-mail address: A.Grant@uea.ac.uk (A. Grant).

https://doi.org/10.1016/j.coastaleng.2023.104328
Received 18 November 2022; Accepted 20 April 2023
Available online 29 April 2023

et al., 2016). However, our ability to synthesise these empirical measurements and models of individual sites into a more generalised conceptual framework and assess the plausibility of some of the very high estimates, has suffered from the lack of a simple theoretical framework giving us a plausible range of values for storm surge attenuation (Leonardi et al., 2018). This also means that we lack clear guidance of what features of the environment should be quantified to aid the interpretation of measured surge attenuation. Here, we develop a simple analytical solution for the movement of a storm surge across a flat surface, including bare mud/sand, grassland/saltmarsh and woodland/mangrove. We use this to assess whether reported values for surge reduction are plausible and, for values which are too high to be physically plausible, critically examine the data on which the claimed reductions are based.

2. A simple analytical model

The flow of water in an open channel can be described using the Manning equation. The depth-averaged horizontal velocity component is u, where

$$u = \left(\frac{1}{n}\right) R^{2/3}\sqrt{S}\,.$$

In the standard formulation, R is the hydraulic radius (cross sectional area/length of wetted perimeter). For an infinite sheet R equals the water depth. Quantity S is often referred to as channel slope, but is more precisely identified as the rate of hydraulic head loss. For flow across a flat impermeable bed, S is *the magnitude of* the slope of the free surface of the water. The choice of sign of the square-root must agree with the observation that u is positive when a wave of positive elevation is advancing from left to right into a region of zero elevation.

The Manning coefficient n quantifies bed friction, and widely used empirical values are: 0.035 for unmown grassland; 0.140–0.150 for woodland (Engineering ToolBox, 2004; Schneider and Arcement, 1984). Values of n for unvegetated surfaces vary between 0.018 and 0.025, depending upon surface roughness (see pages 98–99 and Table 5.5 of Chow, 1959). Rather gentle slopes can generate water velocities that may be surprisingly high for those not familiar with hydraulic calculations. Using the value of the Manning coefficient for grassland given above, a slope of 1m per km generates a velocity of 0.9 m/s (3.2 km/h) in water that is 1 m deep and 2.6 m/s (9.4 km/h) in water that is 5 m deep. Hence, it is immediately apparent that a substantial lowering of water levels as a result from water needing to flow across a flat marsh surface will only occur when flood duration is short or the wetland area is large. For woodland, these velocities are reduced by a factor of 4 (to 0.8 and 2.4 km/h) if we use a Manning coefficient of 0.140. Therefore, mangroves will be more effective than saltmarsh, but the results still imply that substantial and long duration lowering of water level requires wetlands that are several or tens of kilometres wide.

We examine the flow of water over a flat marsh surface at an elevation of $y = 0$. The marsh lies in the region $x > 0$, with the seaward edge is at $x = 0$, as shown in Fig. 1. We assume that the rate of water flow

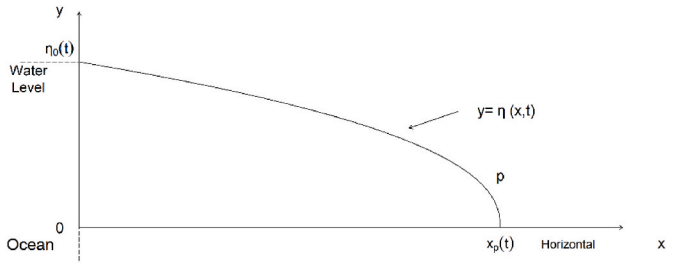

Fig. 1. Schematic diagram of the modelled water surface and model parameters.

onto the marsh has negligible effect on the water level in the region $x < 0$, seawards of the marsh edge.

The leading edge of the encroaching water is at P, with coordinates $x = x_p(t)$, $y = 0$. We denote the depth of water at distance x from the marsh edge and time t as η (x,t), where $0 \le x \le x_p$. For $x > x_p(t)$, the water level is zero. Let the water level at the marsh edge be $\eta_0(t)$, a known function of time and possibly constant.

As the tide rises, the free surface over the marsh rises and the leading edge at P moves to the right. We expect the horizontal component, u, of velocity to be positive, and given by Manning's formula:

$$u(x,t) = \frac{1}{n}\eta^{2/3}\left|\frac{\partial \eta}{\partial x}\right|^{1/2} \tag{1}$$

Where the depth of water η is a function of independent variables x and t and $\left|\frac{\partial \eta}{\partial x}\right|^{1/2}$.

is the square-root of the modulus of the slope of the free surface, under the assumptions that there is zero bed slope and the pressure gradient is only supplied by free-surface inclination. The position of the advancing edge of water, $x = x_p$ at time t, is then:

$$x_p = \frac{1}{n^{2/3}}\frac{3}{2^{2/3}7^{1/3}}\eta_0^{7/9}t^{2/3}. \tag{2}$$

And the water depth at time t and distance x from the marsh edge is given by:

$$\eta(x,t) = \eta_0(t)\left(1 - \frac{x}{x_p(t)}\right)^{3/7} \tag{3}$$

where the factor $\eta_0(t)$ is a prescribed water depth at the marsh edge, and $x \le x_p$ (see appendix A for the derivation of these results). For a steadily rising tide at the marsh edge, we need $\eta_0 = vt$, and we obtain:

$$x_p(t) = \frac{1}{n^{2/3}}\left(\frac{3}{7}\right)^{1/3}\left(\frac{9}{13}\right)^{2/3}v^{7/9}t^{13/9} \tag{4}$$

and

$$\eta(x,t) = vt\left(1 - \frac{x}{x_p(t)}\right)^{3/7} \tag{5}$$

where v is the chosen positive constant rate at which the tide rises in this example.

3. Model predictions

We consider the movement of a flood inland under four different scenarios – a water level at the marsh edge rising at a linear rate, and flood penetration 1 min, 1 h and 4 h after an instantaneous rise in water level. These bracket the range of likely realities as most floods will rise at a rate that decreases as the peak is approached. One hour is a minimum estimate of the duration of a storm surge in areas where surges are comparable or less than the tidal amplitude, as is typical of storm surges on the UK and other North Sea coasts. Penetration over 4 h is chosen to be indicative of impacts of relatively long lasting hurricane driven surges in a microtidal context, such as the Gulf Coast of the USA (e.g. Krauss et al., 2009; McGee et al., 2006). We also use flood penetration over a period of 1 min to give a simplified indicator of the likely effect of vegetation on flooding during tsunamis (c.f. Dahdouh-Guebas et al., 2005; Danielsen et al., 2005; Kathiresan and Rajendran, 2005). For the 2013 North Sea surge, penetration over a 2 h period would probably be most appropriate. Water level peaked at 5.22 m at Immingham but remained above 5 m ODN for 2 h, and at Lowestoft peaked at 3.26m ODN, but was above 3 m for nearly 2 h (Spencer et al., 2015; durations measured from their Figure 5; see also Wadey et al., 2015).

Fig. 2 shows the rate at which the leading edge of the flood moves inland over bare ground (n = 0.018), grass (n = 0.035) and woodland (n

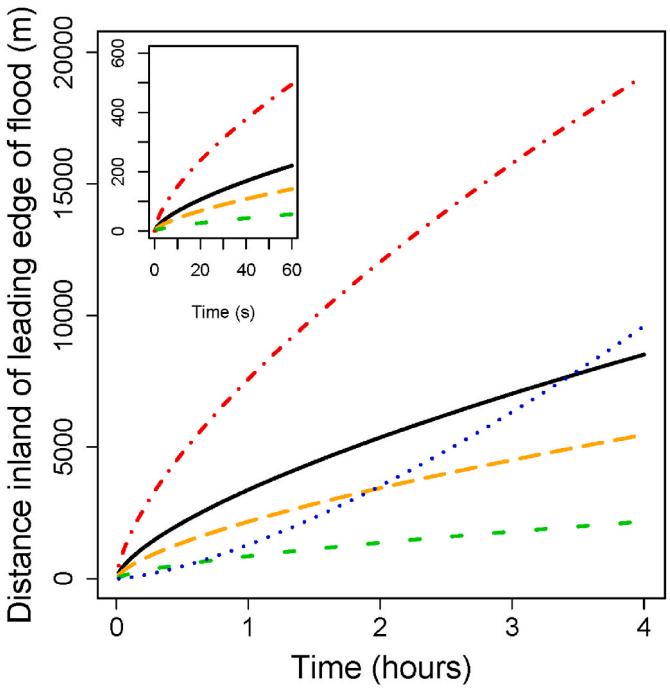

Fig. 2. Movement of leading edge of flood over time for a 1m storm surge over bare ground (black/solid), unmown grassland (orange/long dashes) and woodland/mangrove (green/short dashes), assuming an instantaneous rise in water level at the wetland edge. Red dot/dash line indicates movement of a 5m flood over grassland, and inset shows movement over the initial minute. Blue dotted line show movement of a flood over grassland when water level rises linearly at a rate of 1 m/h.

= 0.140). With a fixed water level of 1m at the edge of the marsh (η_0 = 1m) and a value of 0.035 for n, the Manning coefficient (a value for inmown grass) X_p, the distance inland of the leading edge of the flood will be 142m after 1 min; 2.2 km after 1 h and 5.5 km after 4 h. The distances are 55% higher over bare ground (n = 0.018) and reduced to 39% of these values for woodland (n = 0.140). The distances that a 5m flood would penetrate inland are 3.5 times higher than this, rising from 495m after 1 min to 19.1 km after 4 h for grass. If the water rises at a constant rate, the rate of movement is reduced (blue dotted line), reaching only 1.3 km over grassland after 1 h. After 2 h, this linear rise would lead to a water depth of 2m at the marsh edge and the distance travelled is similar to that resulting from a fixed water depth of 1m.

The relationship between water depth and distance from the marsh edge is plotted in Fig. 3, showing that the slope of the water surface is steepest near the advancing edge at x_p. Water depth is a non-linear

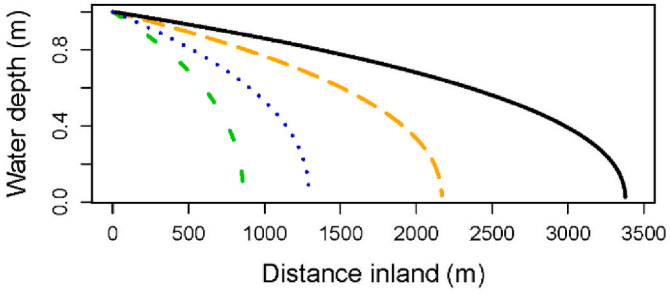

Fig. 3. Pattern of water depth against distance after 1 h of flooding assuming an instantaneous rise of water to 1m above the ground surface at the wetland edge over bare ground (black/solid), unmown grassland (orange/long dashes) and woodland/mangrove (green/short dashes). Dotted blue line shows relationship between water depth and distance for a linear increase in water depth to 1m over 1 h.

function of the proportional distance to x_p, and x_p is a non-linear function of both η_0 and time. Hence, the change in depth across the marsh cannot be exactly characterised by a single reduction in surge height per km. It would be most appropriate to express attenuation as a reduction in the height of a surge of a magnitude and duration that are typical at a location. This should be measured at a distance inland that is a substantial proportion of the area vulnerable to flooding or represents the distance inland of the significant economic assets that are closest to the coast, rather than being extrapolated from measurements made over very short distance (see section 5). The proportional reduction in water depth is greatest for smaller surges and for shorter time periods. However, for values of x up to about 60% of x_p, the relationship between water depth and distance departs only a little from linearity and the *absolute* reduction in water depth is only weakly dependent on storm surge height, although it is strongly dependent on storm surge duration (Fig. 4). Over the first 1 km of the marsh, an instantaneous 1 and 5 m flood would be reduced by 23.3 and 29.4 cm respectively after 1 h, and by 13.7 and 18.2 cm respectively after 2 h. For a surge with a linear rise of 1 m per hour, after 1 h the elevation difference between the edge of the marsh and the 1 km point would be 46.9 cm and 26.6 cm after 2 h. For a linear rise of 2 m/h the difference in water level after 1 h would be 45.2 cm. So flood attenuation can be quite well approximated as an absolute lowering of flood height per km, but it is vital to also state the time period over which this is occurring.

If attenuation rates from modelling studies or empirical measurements are quoted as values per km, they must be measured over horizontal distances of around 1 km. For the majority of the seaward part of the flooded area, the non-linear process that we have described can be approximated as a linear function. But at locations immediately to seawards of the advancing front of the flood, the slope of the water surface is much steeper than the average slope over longer distances (c.f. Fig. 3). In addition, a steep local surface slope can result from water flow across topographic irregularities on the marsh surface, such as small levees along creek banks. It is not meaningful to measure differences in water level over distances of a few tens of metres and then extrapolate these into reductions in flood depth per km, but this is what has been done in a number of recent studies claiming very high reductions in

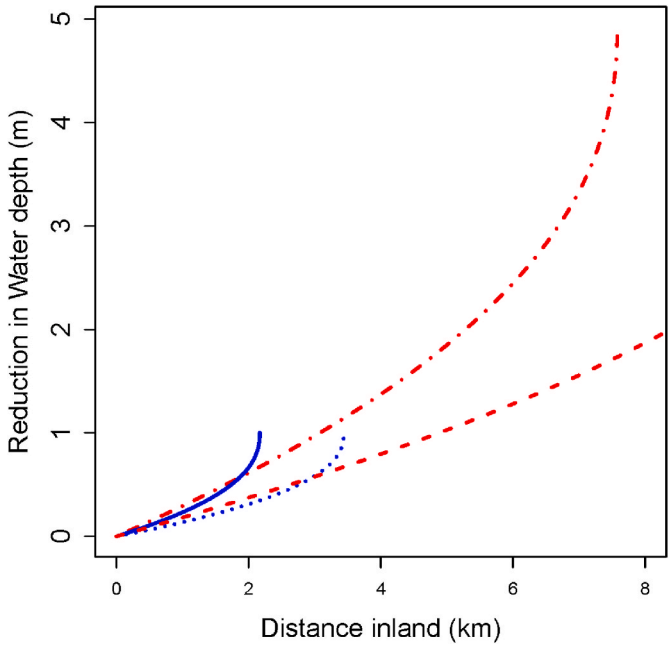

Fig. 4. Reduction in water depth over grass against distance from the marsh edge for a water level that is 1m (blue; solid/dotted lines) and 5m (red; dashed lines) above the marsh surface and times of 1 h (solid and dotted lines) and 2 h (dashed lines).

flood depth (see section 5).

4. When will the model be useful?

The model examines water flow over a flat surface. This will often be a good approximation for the topography of coastal wetlands, which will only be vulnerable to flooding during extreme events if they are at elevations close to normal high water levels (c.f. Alotaibi and Grant, Submitted). However, it will not be a good approximation if the bulk of water flow occurs via tidal channels. Large channels, particularly if these are artificially dredged and/or straightened can transmit flooding large distances inland, such as the suggested role of the Mississippi River Gulf Outlet channel in increasing the severity of flooding during Hurricane Katrina (Shaffer et al., 2009; van Heerden et al., 2009). Our calculations give a maximum value for the lowering of water level, and analyses by Stark et al. suggest that the presence of channels will reduce this by an amount roughly proportional to the ratio of above marsh water volume to the water volume in channels and above the marsh surface (Leonardi et al., 2018; Stark et al., 2016). For the same reasons, if the flood is only a little above the elevation of the marsh surface, then water level at a particular location will be determined by proximity to the drainage network rather than to a steady reduction in water level moving in a landwards direction. This latter mechanism results in substantial differences over short distances between the elevation reached by neap tides on saltmarshes in Norfolk, UK, when flooding occurs almost entirely via channels. On Spring tides, by contrast, the whole marsh surface is submerged and water levels are similar over much larger distances (Mossman et al., 2012). Another departure from the assumption of a uniform flat surface is where one or more elevated ridges run parallel to the shoreline, such as the cheniers characteristic of the coastal plain of Lousiana and elsewhere or shingle/sand ridges that occur on some saltmarshes (Andrews et al., 2000; Augustinus, 1989; McBride et al., 2007; Neal et al., 2002; Otvos, 2012). Where coast-parallel ridges occur, flood behaviour is likely to be dominated by the extent of overtopping of, or penetration through, these barriers, particularly if they have been reinforced as coastal defences or as routes for highways.

5. Comparison with literature values for water level attenuation

Section 3 indicates that water level reductions could be as high as 23–47 cm/km for an event lasting 1 h and 13–27 cm/km after 2 h. A number of recent papers have compiled tables of attenuation rates (Engle, 2011; Glass et al., 2018; Kiesel et al., 2019; Paquier et al., 2017; Stark et al., 2015; Vafeidis et al., 2019; Van Coppenolle et al., 2018). These summarise data from the same primary sources, in some cases relying explicitly on other secondary literature rather than referring to original sources. Some also report their own empirical observations of attenuation rates (Paquier et al., 2017; Kiesel et al., 2019; Stark et al., 2015). Quoted attenuation rates vary from a few cm/km up to a maximum of 270 cm/km (Paquier et al., 2017). The largest reported attenuation rates are examined in Appendix B. In a number of studies, particularly those reporting very high values, the estimated attenuation rates are extrapolated from measurements of water level differences of a few cm between points that are between 20 and 117m apart. This involves multiplication by factors between 8.5 and 50 to express these on a scale of cm per km (Paquier et al., 2017; Kiesel et al., 2019; Stark et al., 2015). The steepest gradient of the water surface occurs at the advancing front of the flood, as illustrated in Fig. 3, but the water surface is non-linear so extrapolating small-scale measurements made here across the whole extent of the flood is very misleading. In one case (Vafeidis et al., 2019), a reduction of 70 cm in water level across a whole estuary with 750 km^2 of wetland (taken from Hu et al., 2015) is misrepresented as a reduction per km. The maximum attenuation, of 29 cm/km, quoted in the abstract of Stark et al. (2016) is the single highest value obtained across several model runs, and occurs in one location in a model scenario in which the marsh is enlarged. The maximum *observed* reduction in tidal height in the same paper is 5 cm/km. Gedan et al. (2011) quote a value of 16.6 cm/km taken from Wamsley et al. but this is the largest value from four model runs. Other model runs gave reductions as small as 4 cm per km, and empirical measurements varied between 4 and 25 cm per km.

Walmsley et al. *(*2010*)* calculated water level attenuation during Hurricane Rita in four locations on the Chenier Plain of Louisiana, using water level measurements recorded by McGee et al. (2006). The greatest attenuation is for a transect near Sabine. Walmsley et al. *(*2010*)* give a water level at the seaward end of transect as 3.3 m (McGee's site LC13; actual measurement 10.62 feet) and water level at the landward end as 2.3 m (McGee's site LC12, 7.52 feet), with a distance between the sites of 4 km. A more precise elevation difference is 94.5 cm, over a distance of 4.22 km (calculated from UTM conversions of latitude/longitude locations in McGee), giving a reduction of 22.4 cm/km. However, site LC13 was located at 29.76407 N 93.75285 E, just to the North of a highway (LA-82) that follows a linear natural ridge that runs East-West at an elevation of 1.9m (Google Maps; https://www.fisheries.noaa.gov/inport/item/53702), with other smaller ridges lying between the two sites. So, a substantial part of the high-water attenuation will be due to the presence of these cheniers, rather than to the presence of vegetation.

6. Conclusions

Our modelling shows that the presence of vegetation substantially reduces the rate at which floods penetrate across low lying coastal wetlands. It also shows that woodland/mangrove is more effective than saltmarsh and other herbaceous vegetation, in line with Gedan et al. (2011) and Krauss et al. (2009). It provides a simple theoretical underpinning for the observations of reduced flood damage on coastlines with vegetated wetlands, particularly mangroves, during tsunamis (Alongi, 2008; Danielsen et al., 2005; Kathiresan and Rajendran, 2005). Flood attenuation due to wetlands is an inherently non-linear process, but away from the advancing flood front can be quite well approximated by a linear relationship in which the reduction in water depth is expressed as an absolute reduction per km, irrespective of surge height. However, it is striking that the literature compiling flood attenuation rates does not systematically discuss duration of the surge. For a surge lasting for 1 h, the water level reduction is approximately 25 cm/km for an instantaneous increase in water level and 45 cm/km for a steadily rising water level, numbers that are approximately halved after 2 h. So the range of 4–25 cm/km given by Gedan et al. (2011) is physically plausible, with lower values being characteristic of longer lasting floods or contexts where wetland drainage channels carry substantial amounts of water in a landwards direction. However, it is clear that some of the larger estimates in the literature are not physically realistic and result from extrapolating measurements of differences in water level between points that are in close proximity. The model also gives guidance as to when it is appropriate to rely on a "bathtub" model of coastal flooding under sea level rise (Anderson et al., 2018; Cooper et al., 2013; Hinkel et al., 2014) by calculating how fast and how far a flood would progress across an area of low lying land and comparing these with the distance of rising ground from the current coastline.

CRediT author statement

Alastair Grant**:** Conceptualization, Methodology, Writing – Original draft preparation, reviewing and editing **Mark Cooker:** Methodology, Formal Analysis, Writing – Original draft preparation, reviewing and editing.

Declaration of competing interest

The authors declare that they have no known competing financial interests or personal relationships that could have appeared to influence the work reported in this paper.

Data availability

No data was used for the research described in the article.

Acknowledgements

This research did not receive any specific grant from funding agencies in the public, commercial, or.

not-for-profit sectors. We are grateful to Robert Nicholls, Tony Davy and Hannah Mossman for comments on draft manuscripts.

Appendix A. an analytical model of storm surge propagation across a flat surface

In order for the free surface to resemble Fig. 1 and to be in accord with Manning's equation, we must have η in the x,t dependence of:

$$\eta(x,t)=\eta_0(t)\left(1-\frac{x}{x_p(t)}\right)^m. \tag{2}$$

The dependence on x in expression (2) is in keeping with Manning's equation for a unidirectional flow without side boundaries. At $x=0$, $\eta=\eta_0(t)$ is the given height of the tide at time t. At the advancing front, $x=x_p(t)$, we want $\eta=0$ to match the surface $y=0$ of the space into which the flow advances. This can only occur if the constant $m>0$. We also need to choose m such that the velocity field in u is finite everywhere, and non-zero at P in order to allow P to move and not be fixed. These considerations will supply a unique value of m. Substituting (2) in (1) gives:

$$u=\frac{1}{n}\eta^{7/6}\frac{m^{1/2}}{x_p{}^{1/2}}\left(1-\frac{x}{x_p(t)}\right)^{\frac{2}{3}m+\frac{m}{2}-\frac{1}{2}}. \tag{3}$$

Now let x increase to x_p so that the bracket tends to zero. If $\frac{2}{3}m+\frac{m}{2}-\frac{1}{2}>0$ then $u\to 0$ and P is fixed in time. On the other hand, if $\frac{2}{3}m+\frac{m}{2}-\frac{1}{2}<0$ then $u=\infty$ at P, which is not realistic. The only remaining possibility is that $\frac{2}{3}m+\frac{m}{2}-\frac{1}{2}=0$ whereupon u can still vary in time but no longer varies with x. From these considerations, the power m must have the unique value

$$m=3/7. \tag{4}$$

Consequently (3) shows that u depends on time only and the water has the same velocity everywhere in the region $0<x<x\_p$:

$$u=\frac{1}{n}\eta_0(t)^{7/6}\left(\frac{3}{7}\right)^{1/2}\frac{1}{x_p(t)^{1/2}}. \tag{5}$$

P is a material fluid particle, so its horizontal velocity $\frac{dx_p}{dt}$ must equal u, as given by (5).

$$\frac{dx_p}{dt}=\frac{1}{n}\eta_0(t)^{7/6}\left(\frac{3}{7}\right)^{1/2}\frac{1}{x_p{}^{1/2}}. \tag{6}$$

This is a separable ordinary differential equation for $x_p(t)$:

$$\int_0^{x_p}x_p{}^{1/2}dx_p=\left(\frac{3}{7}\right)^{1/2}\int_0^t\frac{\eta_0(t)^{7/6}}{n}dt, \tag{7}$$

where the integration limits come from assuming $x_p(0)=0$ at $t=0$. We next carry out the left-hand integration. On the right-hand side, constant n can be taken outside the integral, leaving us with

$$\frac{2}{3}x_p{}^{3/2}=\frac{1}{n}\left(\frac{3}{7}\right)^{1/2}\int_0^t\eta_0(t)^{7/6}dt. \tag{8}$$

Since $\eta_0(t)$ is known, (8) is a way to find x_p as a function of time, and hence the velocity from (5) and the water surface from (2). Two general conclusions from (8) can be drawn. First, so long as $\eta_0(t)$ is positive the integral continues to increase in magnitude, and hence x_p to increase. Second, if $\eta_0(t)$ increases towards some maximum value which it then holds, then x_p continues increasing such that x_p is directly proportional to $t^{2/3}$, and a corresponding diminishing speed directly proportional to $t^{-1/3}$.

We next calculate two examples: first, a constant water level at the marsh edge and second a tide rising linearly in time at the marsh edge. Equation (8) can be used to construct x_p (t) from realistic data of tide height $\eta_0(t)$.

Our first example is unrealistic, except perhaps as a result of a major failure of flood defences some distance away from the marsh, but it gives a maximum possible rate of flooding for a particular height of storm surge. For a constant water level, we set $\eta_0(t)=\eta_0$, a constant for $t>0$.

From (8) we obtain:

$$x_p=\frac{1}{n^{2/3}}\frac{3}{2^{2/3}7^{1/3}}\eta_0{}^{7/9}t^{2/3}. \tag{9}$$

Then (5) gives the water velocity as

$$u=\frac{1}{n^{2/3}}\frac{2^{1/3}}{7^{1/3}}\frac{\eta_0{}^{7/9}}{t^{1/3}}. \tag{10}$$

The velocity starts momentarily infinite over a zero width of fluid. This behaviour is due to the artificially sudden initial increase in water level at $x=0$, but u declines rapidly as t increases from 0. Further, eq. (2) gives the free-surface position for $0<x<x_p$ (t):

$$\eta(x,t) = \eta_0\left(1 - \frac{x}{x_p(t)}\right)^{3/7}. \tag{11}$$

For $x > x_p(t)$, the free surface is assumed to coincide with $y = 0$. Equations (9)–(11) may also be useful for modelling the top of the tide when the water level at $x = 0$ changes little for some time. The front at $x = x_p(t)$ continues to advance according to (9). And (10) shows the water speed diminishes towards zero as t increases. Further, (11) predicts an ever flatter profile of near-constant elevation over a wide range of x. Water depth is equal to 0.84 η_0 at 1/3 of the distance to x_p and to 0.62 η_0 at 2/3 of the distance to x_p.

For our second example, we have a steadily rising tide, $\eta_0(t) = vt$, where $v > 0$ is a constant linear rate at which the tide rises. Then (8) gives:

$$\frac{2}{3}x_p^{3/2} = \frac{1}{n}\left(\frac{3}{7}\right)^{1/2} v^{7/6}\frac{6}{13}t^{13/6}$$

$$x_p(t) = \frac{1}{n^{2/3}}\left(\frac{3}{7}\right)^{1/3}\left(\frac{9}{13}\right)^{2/3} v^{7/9}t^{13/9}. \tag{12}$$

Then the water flows with a velocity given by expression (5):

$$u = \frac{v^{7/9}}{n^{2/3}}\left(\frac{3}{7}\right)^{1/3}\left(\frac{13}{9}\right)^{1/3} t^{4/9}. \tag{13}$$

The flow starts from a state of rest and the velocity continually increases with time. Also, from (2), the free surface position, for $0 < x < x\_p(t)$, is:

$$\eta(x,t) = vt\left(1 - \frac{x}{x_p(t)}\right)^{3/7}. \tag{14}$$

By assumption, for $x > x_p(t)$, the free surface coincides with $y = 0$. If we let the solution (12,13,14) continue up to some instant $t = T$ when the tide ceases to rise and we hold η_0 constant for $t > T$, then three consequences of the modelling (not calculated here) are: $x_p(t)$ continues to increase; u diminishes like eq. (10); and $\eta(t)$ continues to evolve towards a widening near-horizontal water surface, in line with the high-tide level.

Appendix B. Critical assessment of the highest values of water level reductions by wetlands that have been reported in the literature

Water level reduction	Location/event	Source	Comments
Up to 270 cm/km	Observational data, tides and storm surge, Virginia	Paquier et al. (2017)	Measures water level at five locations along a 250m transect. Largest "water level attenuation" is for points 20m apart (Paquier et al., 2017, table 1), and corresponds to an elevation difference of 5.4 cm. During any individual high tide (see their Fig. 7c), water level gradients are initially negative [as water is flooding onto the marsh], then increase, often followed by positive gradients after the time of high tide, as water drains from the marsh and water level at the seaward locations is lower than that of the water remaining on the marsh. What is claimed as "water level attenuation" is the gradient of the surface as water flows onto the marsh and also includes an element that is due to waves. When plotted on an absolute scale (Paquier et al., 2017, Fig. 7a) differences between locations are barely visible.
Up to 100 cm/km	Saltmarsh, Eastern England during normal tides	Kiesel et al. (2019)	Water level was measured at multiple sites, and differences expressed as "HWL attenuation (cm km^{-1})". Largest values of this are 100 cm/km between locations 8 and 9 and 50 cm/km between locations 5 and 6. However, these pairs of points are only 50 and 26m apart respectively, so the "attenuation" corresponds to water height differences are only 5 cm and 1.8 cm. Precision of each elevation measurement is between 2 and 5 cm, so there is no evidence that these height differences are significantly different from zero.
70 cm/km	Modelling study, validated against Hurricane Isaac, Louisiana.	Vafeidis et al. (2019) misrepresenting Hu et al. (2015)	Hu et al. (2015) developed a hydrodynamic model of hurricane driven surges in Breton Sound Estuary, Louisiana, obtaining a close match with measurements for the surge resulting from Hurricane Isaac. The effect of removing vegetation *across the whole* 750 km^2 *of wetland* was estimated to reduce maximum surge height by between 25 and 70 cm. Vafeidis et al. (2019) have taken the highest value in this range and interpreted it as a per km reduction.
70 cm/km	Observational study	Stark et al. (2015)	Highest attenuation rates (Stark et al., 2015, Fig. 4) are measured over short distances. Measurements on their Fig. 1b indicate approximately 57m (between sites 3 and 4); 95 m (sites 3 and 5) and 114 m (sites 8 and 9). "70 cm/km" represents a height difference of approximately 4 cm between sites 57 m apart.
20–50 cm/km	Modelling study, calibrated against data from Hurricane Wilma	Zhang et al. (2012)	Greatest attenuation is for a fast moving hurricane (56 km radius, moving at 40 km/h), where the surge does not have time to penetrate far into the mangroves. With slower moving hurricanes, "surges can still impact the area behind the mangrove zone because the wind has sufficient time to push the ocean water through the mangrove zone". Attenuation is consistent with estimates from our analytical result
29 cm/km	Observational and modelling study, Scheldt Estuary, Netherlands	Stark et al. (2016)	29 cm/km is the highest value found across the whole marsh surface in any of the model runs. The maximum *observed* reduction in tidal height (Stark et al., 2016, Fig. 4) was 5 cm/km.
25 cm/km	Sabine, Louisiana. Hurricane Rita	Wamsley et al. (2010) based on water levels reported by McGee et al. (2006)	Water level at seaward end of transect 3.3 m (McGee's site LC13; actual measurement 10.62 feet); water level at landward end was 2.3 m (McGee's site LC12, 7.52 feet). Actual elevation difference is 94.5 cm, over a distance of 4.22 km (calculated from UTM locations in McGee), giving a reduction of 22.4 cm/km.

(*continued on next page*)

(*continued*)

Water level reduction	Location/event	Source	Comments
			However, site LC13 was located on a highway (LA-82) that follows a linear natural ridge at an elevation of 1.9m (see text for details), with other smaller ridges lying between the two sites. So much of the high water attenuation will be due to land topography rather than vegetation.

References

Alongi, D.M., 2008. Mangrove forests: resilience, protection from tsunamis, and responses to global climate change. Estuar. Coast Shelf Sci. 76 (1), 1–13.

Alotaibi, G. and Grant, A., Submitted. Tidal elevations of UK saltmarshes indicate that their role in reducing coastal flooding has been overestimated.

Anderson, T.R., et al., 2018. Modeling multiple sea level rise stresses reveals up to twice the land at risk compared to strictly passive flooding methods. Sci. Rep. 8 (1), 14484.

Andrews, J.E., et al., 2000. Sedimentary evolution of the North Norfolk barrier coastline in the context of Holocene sea-level change. Geological Society, London, Special Publications 166 (1), 219–251.

Augustinus, P., 1989. Cheniers and chenier plains - a general introduction. Mar. Geol. 90 (4), 219–229.

Barbier, E.B., 2007. Valuing ecosystem services as productive inputs. Econ. Pol. 49, 178–229.

Barbier, E.B., Georgiou, I.Y., Enchelmeyer, B., Reed, D.J., 2013. The value of wetlands in protecting southeast Louisiana from hurricane storm surges. PLoS One 8 (3), e58715.

Chow, V.T., 1959. Open-channel hydraulics. McGraw-Hill Book Co, New York, pp. 680–pp.

Cooper, H.M., Fletcher, C.H., Chen, Q., Barbee, M.M., 2013. Sea-level rise vulnerability mapping for adaptation decisions using lidar DEMS. Prog. Phys. Geogr. Earth Environ. 37 (6), 745–766.

Dahdouh-Guebas, F., et al., 2005. How effective were mangroves as a defence against the recent tsunami? Curr. Biol. 15 (12), R443–R447.

Danielsen, F., et al., 2005. The Asian tsunami: a protective role for coastal vegetation. Science 310 (5748), 643-643.

Engineering ToolBox, 2004. Manning's roughness coefficients [online]. https://www.Engineeringtoolbox.Com/mannings-roughness-d_799.Html (22 Sept. 2022).

Engle, V.D., 2011. Estimating the provision of ecosystem services by Gulf of Mexico coastal wetlands. Wetlands 31 (1), 179–193.

Feagin, R.A., 2008. Vegetation's role in coastal protection. Science 320 (5873), 176–177.

Figueroa-Alfaro, R.W., van Rooijen, A., Garzon, J.L., Evans, M., Harris, A., 2022. Modelling wave attenuation by saltmarsh using satellite-derived vegetation properties. Ecol. Eng. 176.

Garner, A.J., et al., 2017. Impact of climate change on New York city's coastal flood hazard: increasing flood heights from the preindustrial to 2300 CE. Proc. Natl. Acad. Sci. USA 114 (45), 11861–11866.

Gedan, K.B., Kirwan, M.L., Wolanski, E., Barbier, E.B., Silliman, B.R., 2011. The present and future role of coastal wetland vegetation in protecting shorelines: answering recent challenges to the paradigm. Climatic Change 106 (1), 7–29.

Glass, E.M., Garzon, J.L., Lawler, S., Paquier, E., Ferreira, C.M., 2018. Potential of marshes to attenuate storm surge water level in the Chesapeake Bay. Limnol. Oceanogr. 63 (2), 951–967.

Hinkel, J., et al., 2014. Coastal flood damage and adaptation costs under 21st century sea-level rise. Proc. Natl. Acad. Sci. USA 111 (9), 3292–3297.

Hu, K.L., Chen, Q., Wang, H.Q., 2015. A numerical study of vegetation impact on reducing storm surge by wetlands in a semi-enclosed estuary. Coast. Eng. 95, 66–76.

Kathiresan, K., Rajendran, N., 2005. Coastal mangrove forests mitigated tsunami. Estuar. Coast Shelf Sci. 65 (3), 601–606.

Kiesel, J., MacPherson, L.R., Schuerch, M., Vafeidis, A.T., 2022. Can managed realignment buffer extreme surges? The relationship between marsh width, vegetation cover and surge attenuation. Estuar. Coast 45 (2), 345–362.

Kiesel, J., Schuerch, M., Moller, I., Spencer, T., Vafeidis, A., 2019. Attenuation of high water levels over restored saltmarshes can be limited. Insights from Freiston Shore, Lincolnshire, UK. Ecol. Eng. 136, 89–100.

Kirezci, E., et al., 2020. Projections of global-scale extreme sea levels and resulting episodic coastal flooding over the 21st century. Sci. Rep. 10 (1), 11629.

Krauss, K.W., et al., 2009. Water level observations in mangrove swamps during two hurricanes in Florida. Wetlands 29 (1), 142–149.

Kulp, S.A., Strauss, B.H., 2019. New elevation data triple estimates of global vulnerability to sea-level rise and coastal flooding. Nat. Commun. 10 (1), 4844.

Leonardi, N., et al., 2018. Dynamic interactions between coastal storms and salt marshes: a review. Geomorphology 301, 92–107.

Maza, M., Lara, J.L., Losada, I.J., 2022. A paradigm shift in the quantification of wave energy attenuation due to saltmarshes based on their standing biomass. Sci. Rep. 12 (1).

McBride, R.A., Taylor, M.J., Byrnes, M.R., 2007. Coastal morphodynamics and chenier-plain evolution in Southwestern Louisiana, USA: a geomorphic model. Geomorphology 88 (3–4), 367–+.

McGee, B.D., Goree, B.B., Tollett, R.W., Woodward, B.K., Kress, W.H., 2006. Hurricane Rita surge data, Southwestern Louisiana and Southeastern Texas, September to November 2005, p. 220.

Mossman, H.L., Davy, A.J., Grant, A., 2012. Quantifying local variation in tidal regime using depth-logging fish tags. Estuar. Coast Shelf Sci. 96, 122–128.

Neal, A., Richards, J., Pye, K., 2002. Structure and development of shell cheniers in Essex, Southeast England, investigated using high-frequency ground-penetrating radar. Mar. Geol. 185 (3), 435–469.

Otvos, E.G., 2012. Coastal barriers - nomenclature, processes, and classification issues. Geomorphology 139, 39–52.

Paquier, A.E., Haddad, J., Lawler, S., Ferreira, C., 2017. Quantification of the attenuation of storm surge components by a coastal wetland of the US mid Atlantic. Estuar. Coast 40 (4), 930–946.

Pinsky, M.L., Guannel, G., Arkema, K.K., 2013. Quantifying wave attenuation to inform coastal habitat conservation. Ecosphere 4 (8).

Rahmstorf, S., 2017. Rising hazard of storm-surge flooding. Proc. Natl. Acad. Sci. USA 114 (45), 11806–11808.

Resio, D.T., Westerink, J.J., 2008. Modeling the physics of storm surges. Phys. Today 61 (9), 33–38.

Schneider, V.R., Arcement Jr., G.J., 1984. Guide for Selecting Manning's Roughness Coefficients for Natural Channels and Flood Plains.

Shaffer, G.P., et al., 2009. The MRGO navigation project: a massive human-induced environmental, economic, and storm disaster. J. Coast Res. 206–224.

Spencer, T., Brooks, S.M., Evans, B.R., Tempest, J.A., Moller, I., 2015. Southern North Sea storm surge event of 5 December 2013: water levels, waves and coastal impacts. Earth Sci. Rev. 146, 120–145.

Stark, J., Plancke, Y., Ides, S., Meire, P., Temmerman, S., 2016. Coastal flood protection by a combined nature-based and engineering approach: modeling the effects of marsh geometry and surrounding dikes. Estuar. Coast Shelf Sci. 175, 34–45.

Stark, J., Van Oyen, T., Meire, P., Temmerman, S., 2015. Observations of tidal and storm surge attenuation in a large tidal marsh. Limnol. Oceanogr. 60 (4), 1371–1381.

Vafeidis, A.T., et al., 2019. Water-level attenuation in global-scale assessments of exposure to coastal flooding: a sensitivity analysis. Nat. Hazards Earth Syst. Sci. 19 (5), 973–984.

Van Coppenolle, R., Schwarz, C., Temmerman, S., 2018. Contribution of mangroves and salt marshes to nature-based mitigation of coastal flood risks in major deltas of the world. Estuar. Coast 41 (6), 1699–1711.

van Heerden, I.L., et al., 2009. How a navigation channel contributed to most of the flooding of New Orleans during Hurricane Katrina. Publ. Organ. Rev. 9 (4), 291.

Wadey, M.P., et al., 2015. A comparison of the 31 January–1 February 1953 and 5–6 December 2013 coastal flood events around the UK. Front. Mar. Sci. 2.

Wamsley, T.V., Cialone, M.A., Smith, J.M., Atkinson, J.H., Rosati, J.D., 2010. The potential of wetlands in reducing storm surge. Ocean Eng. 37 (1), 59–68.

Zhang, K.Q., et al., 2012. The role of mangroves in attenuating storm surges. Estuar. Coast Shelf Sci. 102, 11–23.

Zhang, W., et al., 2022. The role of seasonal vegetation properties in determining the wave attenuation capacity of coastal marshes: implications for building natural defenses. Ecol. Eng. 175.